Hammett Relationship in Oxidase-Mimicking Metal–Organic Frameworks Revealed through a Protein-Engineering-Inspired Strategy

Jiangjiexing Wu, Zhenzhen Wang, Xin Jin, Shuo Zhang, Tong Li, Yihong Zhang, Hang Xing, Yang Yu, Huigang Zhang, Xingfa Gao,* and Hui Wei*

While the unique physicochemical properties of nanomaterials that enable regulation of nanozyme activities are demonstrated in many systems, quantitative relationships between the nanomaterials structure and their enzymatic activities remain poorly understood, due to the heterogeneity of compositions and active sites in these nanomaterials. Here, inspired by metalloenzymes with well-defined metal–ligand coordination, a set of substituted metal–organic frameworks (MOFs) with similar coordination is employed to investigate the relationship between structure and oxidase-mimicking activity. Both experimental results and density functional theory calculations reveal a Hammett-type structure–activity linear free energy relationship (H-SALR) of MIL-53(Fe) (MIL = Materials of Institute Lavoisier) nanozymes, in which increasing the Hammett σ_m value with electron-withdrawing ligands increases the oxidase-mimicking activity. As a result, MIL-53(Fe) $-NO_2$ with the strongest electron-withdrawing NO_2 substituent shows a tenfold higher activity than the unsubstituted MIL-53(Fe). Furthermore, the generality of H-SALR is demonstrated for a range of substrates, one other metal (Cr), and even one other MOF type (MIL-101). Such biologically inspired quantitative studies demonstrate that it is possible to identify quantitative structure–activity relationships of nanozymes, and to provide detailed insight into the catalytic mechanisms as those in native enzymes, making it possible to use these relationships to develop high-performance nanomaterials.

The shared features of nanomaterials and proteins, such as similar overall size, surface properties, and self-assembly capabilities, have led to the suggestion that nanomaterials could function as protein mimics.[1] Among the nanomaterials, those that exhibit enzyme-like activities, and thus called nanozymes, have recently received considerable attention.[2] Despite impressive progress in developing various types of nanozymes and exploring their potential applications, most studies employ empirical explorations, and rational design strategies have rarely been used in designing high-performance nanozymes.[2a] Very recently, we have shown that for transition metal oxides with an octahedral coordination geometry, their peroxidase-mimicking activities exhibited a volcano-type dependence on the e_g occupancies of the corresponding transition metals.[3] Nevertheless, for most of the currently developed nanozymes, such explicit quantitative structure–activity relationships have not been identified.[2a] This lack of advancement is mainly due to the composition heterogeneity and

Dr. J. Wu, X. Jin, S. Zhang, T. Li, Y. Zhang, Prof. H. Zhang, Prof. H. Wei
College of Engineering and Applied Sciences
Nanjing National Laboratory of Microstructures
Jiangsu Key Laboratory of Artificial Functional Materials
Nanjing University
Nanjing, Jiangsu 210093, China
E-mail: weihui@nju.edu.cn
Dr. Z. Wang, Prof. X. Gao
Laboratory of Theoretical and Computational Nanoscience
CAS Key Laboratory of Nanophotonic Materials and Devices
CAS Key Laboratory for Biomedical Effects of Nanomaterials
and Nanosafety
National Center for Nanoscience and Technology
Chinese Academy of Sciences
Beijing 100190, China
E-mail: gaoxf@nanoctr.cn

Prof. H. Xing
Institute of Chemical Biology and Nanomedicine
State Key Laboratory of Chemo/Biosensing and Chemometrics
College of Chemistry and Chemical Engineering
Hunan University
Changsha, Hunan 410082, China
Prof. Y. Yu
Department of Biochemical Engineering and Institute
for Synthetic Biosystem
School of Chemistry and Chemical Engineering
Beijing Institute of Technology
Beijing 100081, China
Prof. H. Wei
State Key Laboratory of Analytical Chemistry for Life Science and State
Key Laboratory of Coordination Chemistry
Chemistry and Biomedicine Innovation Center (ChemBIC)
School of Chemistry and Chemical Engineering
Nanjing University
Nanjing, Jiangsu 210023, China

ambiguity in the active sites of nanomaterials, making the identification of the number, location, and nature of active centers very challenging, which in turn hamper the elucidation of quantitative structure–activity relationships and thus limit the rational design of high-performance nanozymes.

In contrast, protein enzymes have well-defined active sites and nearby microenvironments/residues (e.g., primary and secondary coordination spheres) that can be rationally engineered to investigate the structure–activity relationships. Protein engineering has gained insight into the correlation between catalytic efficiency and the structures of mutated enzymes.[4] As in-depth knowledge of protein engineering and advanced technologies become available, more advanced engineering, such as those employing unnatural amino acids and non-native cofactors, can be introduced to design enzymes with better catalytic activity.[5] For example, in a functional model of oxidase, incorporation of tyrosine analogs with decreased pK_a values resulted in a linear enhancement of the O_2 reduction activities, allowing the pK_a-dependent activity regulation of oxidase and revealing the role of active site tyrosine in oxidase reaction as well.[6]

Inspired by the success of enzyme engineering, we envision that nanomaterials with similar well-defined structures would enable us to explore the structure–activity relationship of nanozymes and further rationally design high-performance nanozymes. One emerging category of nanozymes comprises the metal–organic frameworks (MOFs), which are 3D networks of metal ions linked by multidentate organic linkers.[7] Therefore, in this work, MIL-53(Fe) (MIL = Materials of Institute Lavoisier), benefitting from its broad variety of functional ligands and Fe metal node widely used in metalloenzymes, was chosen as a model system to study the relationship between the structure and its oxidase-mimicking activity (**Figure 1**a). Through systematically changing the linker substituent X in MIL-53(Fe) −X (X = NH$_2$, CH$_3$, H, OH, F, Cl, Br, and NO$_2$), the oxidase-mimicking activities can be tuned accordingly. Specifically, the oxidase-mimicking activity of MIL-53(Fe) −X-based nanozymes is correlated to Hammett σ_m values[8] of the linker substituent X, which quantify the electronic effects of substituents in molecular chemistry. In particular, a Hammett-type structure–activity linear free energy relationship (H-SALR) is also revealed. This concept is also supported by density functional theory (DFT) calculations. Moreover, the identified structure–activity relationship is found to be general to other MOF-based nanozymes.

The MIL-53(Fe) −X frameworks, constructed through the coordination between FeO$_6$ octahedrons and unsubstituted/substituted 1,4-benzenedicarboxylic acid (BDC) ligands (Figure 1), were synthesized via a solvothermal method (Figure S1, Supporting Information). The resulting products were characterized by powder X-ray diffraction (PXRD) measurement, confirming the structure of MIL-53(Fe) (Figure S2, Supporting Information).[9] X-ray photoelectron spectra (XPS) indicated the presence of Fe, C, and O in all of the MOFs, and N, F, Cl, and Br in the NH$_2$-, NO$_2$-, F-, Cl-, and Br-substituted MOFs (Figure S3a, Supporting Information). Then, the oxidase-mimicking activities (**Figure 2**a) of the MOFs were evaluated through monitoring the absorption peak at 652 nm of oxidized 3,3′,5,5′-tetramethylbenzidine (TMB). As shown in Figure 2b, except for MIL-53(Fe) −NH$_2$, which exhibited nearly negligible
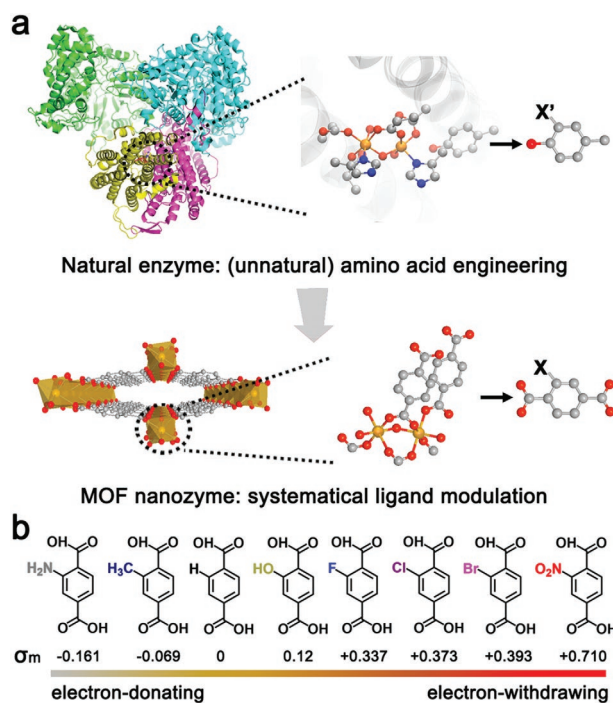

Figure 1. a) Protein-engineering-inspired MOF nanozyme modulation. Illustration of modulating catalytic activity of MOF nanozyme with substituted organic linkers, which is inspired by the catalytic activity modulation of natural enzyme via a protein engineering strategy. The protein drawing is based on the crystal structure of an oxidoreductase (PDB ID: 6W4X). The Fe center and amino acids are displayed as a ball-and-stick representation. The Fe metal node and organic linkers for MOF drawing are also marked as a ball-and-stick representation. Fe: orange; O: red; C: gray; and N: blue. b) Substituted organic linkers with different electronic modulation capabilities used in this work. The Hammett σ_m values were obtained from ref. [8].

activity, all the MIL-53(Fe) −X MOFs exhibited oxidase-mimicking catalytic activity. The oxidase-mimicking activity of MIL-53(Fe) was dramatically enhanced after F, Cl, Br, and NO$_2$ substitution. Remarkably, a more than tenfold increase in the oxidase-mimicking activity was obtained upon the introduction of a NO$_2$ group into the MIL-53(Fe) MOF (Figures S4 and S5, Supporting Information). The study of O_2-dependent catalytic activities of the MIL-53(Fe) −X MOFs further validated their oxidase-mimicking properties (Figure S6, Supporting Information).

To confirm that the oxidase-mimicking activity was from the MOFs rather than the substituted ligands, control experiments with only these substituted ligands added to oxidase-mimicking catalytic reaction solutions were performed. As shown in Figure S7 (Supporting Information) under the same conditions, none of these substituted ligands alone exhibited oxidase-mimicking activity, confirming that the oxidase-mimicking activity originated from the MOFs. A careful study of the thermogravimetric analysis results shown in Figure S8 and Table S1 (Supporting Information), demonstrated that there was linker deficiency in these MOF structures. As a result, we reasoned that unsaturated sites on metal nodes existed in MIL-53(Fe) −X MOFs and functioned as the active sites, which was consistent with the active site in natural oxidase.[10] In addition, the
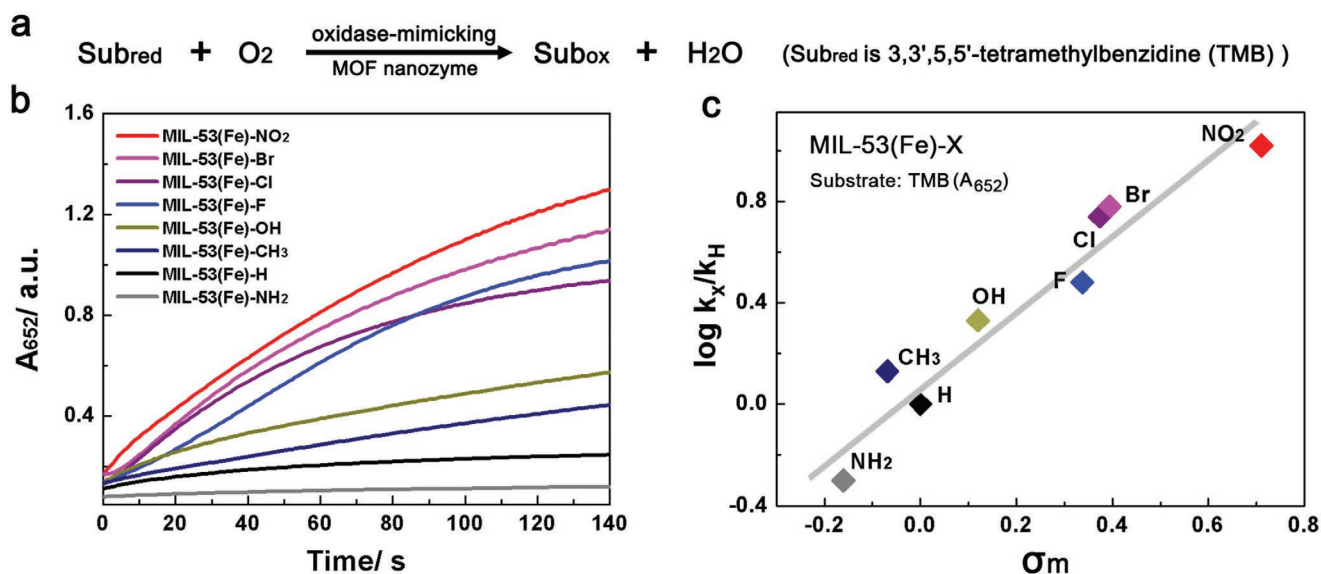
ADVANCED
SCIENCE NEWS
www.advancedsciencenews.com

ADVANCED
MATERIALS
www.advmat.de

a

Sub$_{red}$ + O$_2$ $\xrightarrow[\text{MOF nanozyme}]{\text{oxidase-mimicking}}$ Sub$_{ox}$ + H$_2$O   (Sub$_{red}$ is 3,3',5,5'-tetramethylbenzidine (TMB))

Figure 2. a) Oxidation of a substrate (i.e., TMB) with O$_2$ catalyzed by oxidase-mimicking MOF nanozymes, producing oxidized product and H$_2$O. b) Time evolution of absorbance at 652 nm (A_{652}) for monitoring the oxidase-mimicking catalytic activities of MIL-53(Fe) −X MOFs, under the condition of 50×10^{-3} M NaOAc buffer (pH = 4.5) containing 1×10^{-3} M TMB substrate at room temperature. MIL-53(Fe) was written as MIL-53(Fe) −H for a clear view of the substituent. c) Catalytic TMB oxidation activities of MIL-53(Fe) −X MOFs plotted as a function of Hammett σ_m values of the linker substituent X. Values of k_X were calculated from initial kinetic observations. The gray line is shown as a visual guide only. X = NH$_2$, CH$_3$, H, OH, F, Cl, Br, and NO$_2$.

particle size independence of the oxidase-mimicking activity of MIL-53(Fe) −X was also revealed in Figures S9 and S10 (Supporting Information), implying that all the catalytic sites participated and contributed during the oxidase-mimicking catalytic reactions.[11] The large channels present in MIL-53(Fe) made the catalytic sites accessible to the substrates (Figure S11, Supporting Information).[12]

The above analysis suggested that the substituent effect was the main reason for the distinct difference in the oxidase-mimicking activity of MIL-53(Fe) −X MOFs. A detailed XPS study for Fe 2p in Figure S3b (Supporting Information) showed different binding energies for different substituents, which clearly indicated the modulation of electronic structures of metal nodes by the substituents. Although the variations for some substituents were small, the overall trend illustrated that the presence of an electron-withdrawing group, especially a nitro group—the strongest typical electron-withdrawing group, clearly shifted the binding energy to a lager value, agreeing well with a previous report.[13] When using Hammett's σ_m values to describe the electronic effects of these substituted ligands, an H-SALR was identified (Figure 2c), which is a typical one in the field of quantitative structure–activity relationship. The positive correlation indicated that a negative charge developed during the rate-limiting step of the reaction. Therefore, the electron-withdrawing ligand made the metal node more electron deficient, and thus an even better electron sponge, facilitating electron transfer among the substrates, oxygen, and the MOFs. Moreover, the facilitation of electron transfer by the electron-withdrawing ligand was further supported by the increased reduction potentials of MIL-53(Fe) −X with electron-withdrawing ligands (Figure S12, Supporting Information), consistent with a literature report that a higher reduction potential resulted in a faster electron transfer from

the substrate, and thus was responsible for a higher oxidase-mimicking activity.[5b]

To provide theoretical basis for the H-SALR, DFT calculations were performed to understand the structures and energies for MIL-53(Fe) −X and to reveal the key intermediates involved in their oxidase-mimicking catalyses. All the nanozymes were modeled by a slab derived from the bulk crystal structure of MIL-53(Fe) −X (Figure S13, Supporting Information). In the slab, each iron atom coordinated with five oxygen atoms, representing the coordinatively unsaturated irons in the nanozymes. According to the calculated results, the electron spins of all neighboring irons in the MIL-53(Fe) −X slabs preferred an anti-ferromagnetic coupling (Figure S14, Supporting Information). Both the highest occupied molecular orbital (HOMO) and lowest unoccupied molecular orbital (LUMO) were mainly located on the d-orbitals of irons, suggesting irons to be the most probable catalytic centers (Figure S15, Supporting Information). The energy of LUMOs, which signified the reduction potentials of the nanozymes, exhibited a linear relationship with the Hammett σ_m value of substituent X (Figure S16, Supporting Information), in good agreement with the experiment (Figure S12, Supporting Information). It is also agreed with the knowledge that electron-donating and -withdrawing groups raise and lower the frontier molecular orbital energies, respectively.[14] The π-conjugation between substituent X and irons, which was known as the mesomeric substituent effect,[15] was the dominant way through which the substituent adjusted the orbital energy associated with iron (Figure S17, Supporting Information). The inductive substituent effect, which was a short-range electronic effect caused by the difference in atomic electronegativity,[15] played a minor role because all substituent Xs were spatially separated from irons too far, by at least four atoms (one O and three C atoms).
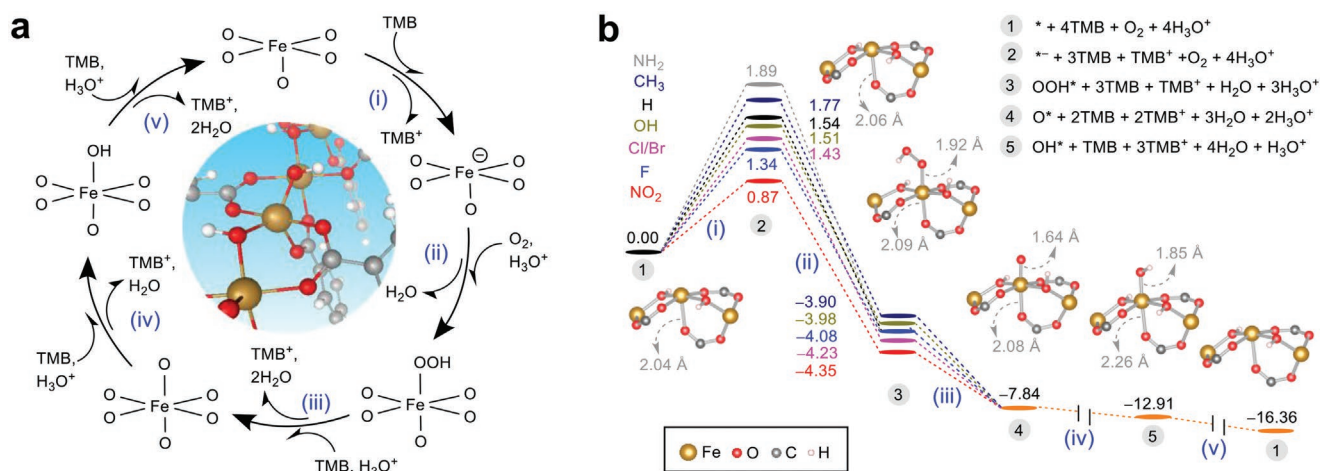
ADVANCED
SCIENCE NEWS
www.advancedsciencenews.com

ADVANCED
MATERIALS
www.advmat.de

Figure 3. a) Proposed catalytic cycle for the oxidation of TMB to TMB$^+$ with MIL-53(Fe) −X as oxidase mimics. b) Energies (in eV) of key intermediates in the catalytic cycle of (a) for MIL-53(Fe) −X. X = NH$_2$, CH$_3$, H, OH, F, Cl, Br, and NO$_2$. In (b), the asterisk * represents the catalytic center, and the structures of the intermediates near the catalytic centers are shown for X = NO$_2$.

Based on the above calculations, we proposed a catalytic mechanism for the oxidase-mimicking activity of MIL-53(Fe) −X, similar to those of natural oxidases (**Figure 3**a).[16] This mechanism mainly consisted of five reaction steps: i) the transfer of an electron from TMB to MIL-53(Fe) −X to increase the affinity of the nanozyme toward O$_2$; ii) the protonation-coupled adsorption of an O$_2$ molecule on the iron center to give the OOH adsorbate; and iii–v) three consecutive protonation-coupled electron transfer steps to reduce the OOH adsorbate and simultaneously to regenerate the catalytic center. Figure 3b plotted the energies for the intermediates in the catalytic cycles. For all MIL-53(Fe) −X nanozymes, step (i) was endothermic with a positive reaction energy (E_r); steps (ii)–(v) were all highly exothermic with negative $E_r < -1.5$ eV. Therefore, step (i) was the most probable rate-determining step, whose energy barrier E_b determined the overall reaction rate. This meant that a nanozyme with a lower E_b would have a higher oxidase-mimicking activity and vice versa. According to Figure 3b, the E_r for step (i) increased in the order of NO$_2$ < F < Cl, Br < OH <

H < CH$_3$ < NH$_2$. According to the linear scaling relationship between E_b and E_r, i.e., the Brønsted–Evans–Polanyi (BEP) relation,[17] E_b for step (i) should have the same order as E_r. Such an increasing E_b order excellently agreed with the inverse oxidase-mimicking activity order experimentally found for MIL-53(Fe) −X (Figure 2c). Notably, step (i) was a net electron transfer process, and its E_r linearly scaled with the reduction potential of the nanozyme. And further because of the linear relationship between E_b and E_r (the BEP relationship)[17] and that between reduction potential and Hammett σ_m value, E_b should also be linearly scaled with the Hammett σ_m value, which explained the H-SALR of the oxidase-mimicking activity.

To evaluate whether this H-SALR is a general phenomenon, we studied other oxidase substrates, including 2,2′-azino-bis(3-ethylbenzothiazoline-6-sulfonic acid) (ABTS) and 2,4-dichlorophenol (2,4-DP), MIL-53 with other metal nodes (such as Cr), and even other types of MOFs (such as MIL-101(Fe)). As shown in **Figure 4**a and in Figure S18 (Supporting Information), when ABTS was used instead of TMB as the substrate for oxidation, a
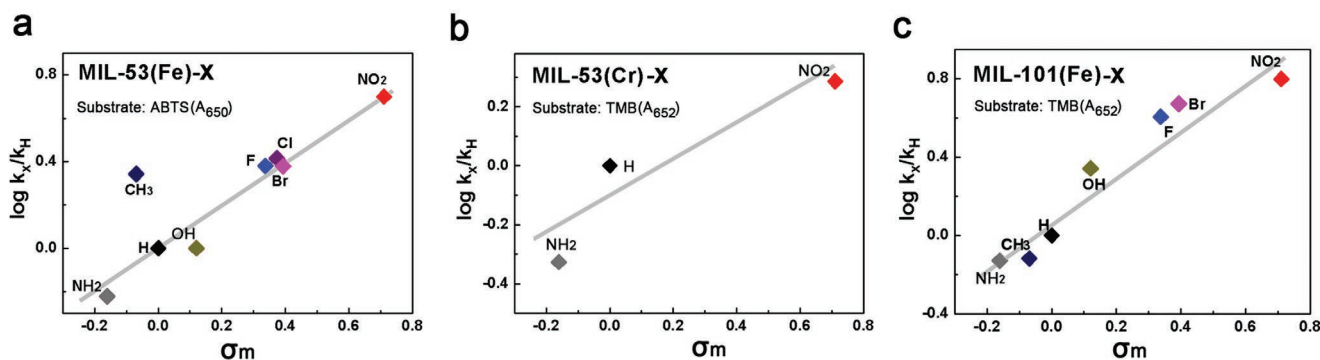

Figure 4. a) Generality of H-SALR to one other substrate (ABTS). Catalytic ABTS oxidation activity of MIL-53(Fe) −X (X = NH$_2$, CH$_3$, H, OH, F, Cl, Br, and NO$_2$) plotted as a function of Hammett σ_m values of the linker substituent X. b) Generality of H-SALR to one other metal (Cr). Catalytic TMB oxidation activity of MIL-101(Cr)-X MOFs (X = NH$_2$, H, and NO$_2$) plotted as a function of Hammett σ_m values of the linker substituent X. c) Generality of H-SALR to one other MOF (MIL-101). Catalytic TMB oxidation activity of MIL-101(Fe) −X MOFs (X = NH$_2$, CH$_3$, H, OH, F, Br, and NO$_2$) plotted as a function of Hammett σ_m values of the linker substituent X. The gray lines are shown as visual guides only.

similar H-SALR was identified, where the electron-withdrawing groups, especially NO_2, significantly enhanced the oxidase-mimicking catalytic activity. Considering that the oxidation rate of ABTS is often utilized to determine the catalytic activity of the enzyme laccase, these substituted MIL-53(Fe) −X MOFs could be defined as laccase mimics.[18]

In addition to oxidizing ABTS, laccases also oxidize phenols and play an important role in environmental protection by removing these harmful compounds. According to the revealed H-SALR of MIL-53(Fe) −X MOFs, we hypothesized that among all the substituted MOFs, MIL-53(Fe) −NO_2 should be the most efficient laccase mimic for phenol oxidation and removal. Notably, the experimental results of 2,4-DP oxidation shown in Figure S19 (Supporting Information) verified this hypothesis. Furthermore, the MIL-53 MOF with the other metal node (i.e., Cr here) was also tested (Figures S20 and S21, Supporting Information). Due to the relatively low oxidase-mimicking activity of MIL-53(Cr), only the nitro and amine groups were utilized to functionalize MIL-53(Cr) for comparison (Figure S22, Supporting Information). The electron-withdrawing NO_2 group also enhanced the oxidase-mimicking catalytic activity in the Cr MOF (Figure 4b). In addition, this H-SALR was even applicable to another type of MOF, MIL-101(Fe) −X (Figure 4c; Figures S23 and S24, Supporting Information). Therefore, according to the above observations, the generality of H-SALR led to the conclusion that being independent of the type of substrate, metal node, and MOF, the electronic effect of substituted ligands is nearly universal and dominate for oxidase-mimicking activity modulation.

In summary, by employing a set of substituted MOFs to imitate the metal–ligand coordination of natural redox enzymes, we have successfully revealed a Hammett-type structure–activity linear free energy relationship for oxidase-mimicking nanozymes, i.e., increasing the Hammett σ_m value by incorporating an electron-withdrawing ligand leads to an increase in the oxidase-mimicking activity. Additionally, both the experimental results and DFT calculations have provided better understanding of the catalytic mechanism. By reaching similarly high level of quantitative understanding of structure–function relationship of nanozymes as in native enzymes, this work offers exciting new perspectives and opportunities to apply more biomimetic methods for studying the structure–activity relationships of other nanozymes and to guide the design of high-performance nanomaterials.

Supporting Information

Supporting Information is available from the Wiley Online Library or from the author.

[1] N. A. Kotov, *Science* **2010**, *330*, 188.

[2] a) J. Wu, X. Wang, Q. Wang, Z. Lou, S. Li, Y. Zhu, L. Qin, H. Wei, *Chem. Soc. Rev.* **2019**, *48*, 1004; b) L. Z. Gao, J. Zhuang, L. Nie, J. B. Zhang, Y. Zhang, N. Gu, T. H. Wang, J. Feng, D. L. Yang, S. Perrett, X. Y. Yan, *Nat. Nanotechnol.* **2007**, *2*, 577; c) F. Natalio, R. André, A. F. Hartog, B. Stoll, K. P. Jochum, R. Wever, W. Tremel, *Nat. Nanotechnol.* **2012**, *7*, 530; d) G. Y. Tonga, Y. Jeong, B. Duncan, T. Mizuhara, R. Mout, R. Das, S. T. Kim, Y.-C. Yeh, B. Yan, S. Hou, V. M. Rotello, *Nat. Chem.* **2015**, *7*, 597; e) Z. Zhang, X. Zhang, B. Liu, J. Liu, *J. Am. Chem. Soc.* **2017**, *139*, 5412; f) M. A. Komkova, E. E. Karyakina, A. A. Karyakin, *J. Am. Chem. Soc.* **2018**, *140*, 11302; g) C. N. Loynachan, A. P. Soleimany, J. S. Dudani, Y. Lin, A. Najer, A. Bekdemir, Q. Chen, S. N. Bhatia, M. M. Stevens, *Nat. Nanotechnol.* **2019**, *14*, 883; h) L. Huang, J. Chen, L. Gan, J. Wang, S. Dong, *Sci. Adv.* **2019**, *5*, eaav5490.

[3] X. Wang, X. J. Gao, L. Qin, C. Wang, L. Song, Y.-N. Zhou, G. Zhu, W. Cao, S. Lin, L. Zhou, K. Wang, H. Zhang, Z. Jin, P. Wang, X. Gao, H. Wei, *Nat. Commun.* **2019**, *10*, 704.

[4] I. R. Greig, *Chem. Soc. Rev.* **2010**, *39*, 2272.

[5] a) J. Liu, S. Chakraborty, P. Hosseinzadeh, Y. Yu, S. Tian, I. Petrik, A. Bhagi, Y. Lu, *Chem. Rev.* **2014**, *114*, 4366; b) A. Bhagi-Damodaran, M. Kahle, Y. Shi, Y. Zhang, P. Ädelroth, Y. Lu, *Angew. Chem., Int. Ed.* **2017**, *56*, 6622.

[6] Y. Yu, X. Lv, J. Li, Q. Zhou, C. Cui, P. Hosseinzadeh, A. Mukherjee, M. J. Nilges, J. Wang, Y. Lu, *J. Am. Chem. Soc.* **2015**, *137*, 4594.

[7] a) H. Deng, C. J. Doonan, H. Furukawa, R. B. Ferreira, J. Towne, C. B. Knobler, B. Wang, O. M. Yaghi, *Science* **2010**, *327*, 846; b) M. Zhao, K. Yuan, Y. Wang, G. Li, J. Guo, L. Gu, W. Hu, H. Zhao, Z. Tang, *Nature* **2016**, *539*, 76; c) Y. Chen, S. Ma, T. Dalton, **2016**, *45*, 9744; d) C. M. McGuirk, M. J. Katz, C. L. Stern, A. A. Sarjeant, J. T. Hupp, O. K. Farha, C. A. Mirkin, *J. Am. Chem. Soc.* **2015**, *137*, 919; e) K. Chen, C.-D. Wu, *Coord. Chem. Rev.* **2019**, *378*, 445; f) S. Kitagawa, *Acc. Chem. Res.* **2017**, *50*, 514; g) S. M. J. Rogge, A. Bavykina, J. Hajek, H. Garcia, A. I. Olivos-Suarez, A. Sepulveda-Escribano, A. Vimont, G. Clet, P. Bazin, F. Kapteijn, M. Daturi, E. V. Ramos-Fernandez, F. X. Llabres i Xamena, V. Van Speybroeck, J. Gascon, *Chem. Soc. Rev.* **2017**, *46*, 3134; h) M. Zhang, Z.-Y. Gu, M. Bosch, Z. Perry, H.-C. Zhou, *Coord. Chem. Rev.* **2015**, *293–294*, 327; i) I. Nath, J. Chakraborty, F. Verpoort, *Chem. Soc. Rev.* **2016**, *45*, 4127.

[8] C. H. Hansch, A. Leo, *Substituent Constants for Correlation Analysis in Chemistry and Biology*, Wiley, New York **1979**.

[9] P. Horcajada, C. Serre, G. Maurin, N. A. Ramsahye, F. Balas, M. Vallet-Regí, M. Sebban, F. Taulelle, G. Férey, *J. Am. Chem. Soc.* **2008**, *130*, 6774.

[10] S. Yoshikawa, A. Shimada, *Chem. Rev.* **2015**, *115*, 1936.

[11] F. Vermoortele, M. Vandichel, B. Van de Voorde, R. Ameloot, M. Waroquier, V. Van Speybroeck, D. E. De Vos, *Angew. Chem., Int. Ed.* **2012**, *51*, 4887.

[12] C. Serre, F. Millange, C. Thouvenot, M. Noguès, G. Marsolier, D. Louër, G. Férey, *J. Am. Chem. Soc.* **2002**, *124*, 13519.

[13] J. Liu, Z. Li, X. Zhang, K.-i. Otake, L. Zhang, A. W. Peters, M. J. Young, N. M. Bedford, S. P. Letourneau, D. J. Mandia, J. W. Elam, O. K. Farha, J. T. Hupp, *ACS Catal.* **2019**, *9*, 3198.

[14] Y. Mao, M. Head-Gordon, Y. Shao, *Chem. Sci.* **2018**, *9*, 8598.

[15] R. Barret, in *Therapeutical Chemistry* (Ed: R. Barret), Elsevier, San Diego, CA, USA **2018**, p. 21.

[16] D. Bloch, I. Belevich, A. Jasaitis, C. Ribacka, A. Puustinen, M. I. Verkhovsky, M. Wikström, *Proc. Natl. Acad. Sci. USA* **2004**, *101*, 529.

[17] S. Wang, B. Temel, J. Shen, G. Jones, L. C. Grabow, F. Studt, T. Bligaard, F. Abild-Pedersen, C. H. Christensen, J. K. Nørskov, *Catal. Lett.* **2011**, *141*, 370.

[18] C. Johannes, A. Majcherczyk, *J. Biotechnol.* **2000**, *78*, 193.

2005024 (6 of 6)